Application of a Laser-Wakefield Driven Monochromatic Photon Source to Nuclear Resonance Fluorescence

W.J. Walsh, S.D. Clarke, S.A. Pozzi, *IEEE Member*, N. Cunningham, S. Banerjee, D. Umstadter

Abstract – **Nuclear resonance fluorescence is of particular interest to the detection of special nuclear material (SNM) where isotopic characterization is paramount. In addition to photons emitted by resonance de-excitation, there will also be a significant amount of backscattered photons that will distort the NRF signal. The backscattered spectra must be characterized in order to design a detection system that maximizes the material identification probability. However, to our knowledge the cross-sections for nuclear resonance absorption do not exist in any version MCNP. Therefore, a novel method is applied here to reproduce the measured results from Bertozzi et al. using bremsstrahlung X-rays. The NRF signal this source was compared with the response from the University of Nebraska (UNL) quasi-monochromatic X-ray source to compare the performance on a per source photon basis. An absolute comparison of each source is left for future work. The results of the simulations show that the UNL source would have a higher efficiency on a per source photon basis by a factor of approximately 170.**

I. Introduction

THE Diocles laser facility at The University of Nebraska-Lincoln (UNL) is a 100-TW, 30-fs pulsed Ti:sapphire laser system. Diocles routinely provides electron beams exhibiting high energy (up to 400 MeV), high beam charge (approximately 0.1 nC) and narrow energy width (~10%) [1]. These electrons may be scattered off of residual laser light, producing quasi-monochromatic X-rays with energy and spectral width that are directly related to those of the electron beam. This approach presents the possibility of producing a tunable, quasi-monochromatic X-ray source that has promising applications in nuclear material detection. By using a quasi-monochromatic light source at the appropriate energy it is possible to excite nuclei by resonance photon absorption. The excited nucleus then de-excites by emitting a photon of nearly identical energy. This process of excitation and de-excitation is known as nuclear resonance fluorescence (NRF).

NRF spectroscopy is a promising technique that can exploit nuclear physics in order to characterize an unknown isotope [2]. It is possible to analyze these emissions and determine the identity of an unknown material because every nucleus has distinct energy levels. This technique is of particular interest to the detection of special nuclear material (SNM) where isotopic characterization is paramount.

The ability to tune the UNL X-ray source provides much-needed versatility and addresses one potential shortcoming of traditional bremsstrahlung X-ray sources for NRF spectroscopy. Namely bremsstrahlung sources are wide-band and, as a result, produce large amounts of background radiation and excess bystander dose. A tunable source may be used to selectively excite individual nuclei while minimizing bystander dose.

Using a quasi-monochromatic photon source will be more efficient than using a traditional bremsstrahlung source for a single resonance excitation. The energy width of a nuclear resonance is very narrow: approximately 10^{-1} eV. The ability to positively identify SNM relies on the excitation of the target nuclei by the source photons. Therefore, it is beneficial for the interrogation source to emit as many photons within the nuclear resonance as possible. Using a monoenergetic source increases the percent of photons that lie in the resonance over a bremsstrahlung source. Because of this, the probability of exciting the desired resonance per source photon is expected to be higher for the monochromatic source than a traditional bremsstrahlung source.

II. Measured Data

In order to evaluate the simulation method, the results of an NRF experiment will be compared to the simulated results using the novel simulation method. The experiment was performed by Bertozzi et al. at the High Voltage Research Laboratory (HVRL) at the Massachusetts Institute of Technology (MIT) [3]. The experimental setup is shown in Fig. 1.

Manuscript submitted on November 13, 2009.

W. J. Walsh is with the Department of Nuclear Engineering and Radiological Sciences of the University of Michigan, Ann Arbor, MI 48109 USA (e-mail: wwalsh@umich.edu).

S. D. Clarke is with the Department of Nuclear Engineering and Radiological Sciences of the University of Michigan, Ann Arbor, MI 48109 USA (tel: 734-615-7830, e-mail: clarkesd@umich.edu).

S. A. Pozzi is with the Department of Nuclear Engineering and Radiological Sciences of the University of Michigan, Ann Arbor, MI 48109 USA (tel: 734-615-4970, e-mail: pozzisa@umich.edu).

N. Cunningham is with the Physics and Astronomy Department of the University of Nebraska, Lincoln, NE 68588 USA (e-mail: ncunningham2@unl.edu).

S. Banerjee is with the Physics and Astronomy Department of the University of Nebraska, Lincoln, NE 68588 USA (e-mail: sbanerjee2@unl.edu).

D. Umstadter is with the Physics and Astronomy Department of the University of Nebraska, Lincoln, NE 68588 USA (tel: 402-472-8115, e-mail: dpu@unlserve.unl.edu).

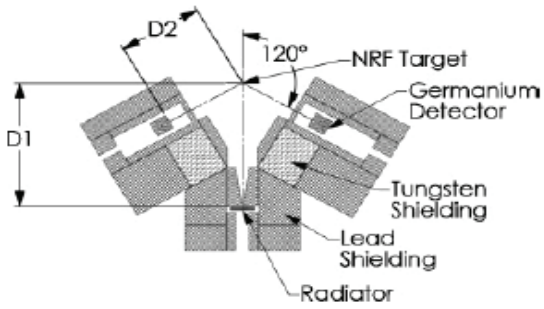

Fig. 1. Experimental setup of the NRF experiment performed by Bertozzi et al [3].

A 2.2-MeV electron beam was directed at the bremsstrahlung radiator. The bremsstrahlung radiator consists of a 0.102-cm thick layer of gold backed by 1-cm thick layer of copper. The gold produces the bremsstrahlung X-rays and the copper conducts heat away from the gold, and attenuates any residual electrons. The photons then travel through a lead collimator with a 2.5-degree half-angle. The NRF target is located 60 cm from the bremsstrahlung radiator. Two high purity germanium (HPGe) detectors are located 45 cm from the NRF target at an angle of plus-and-minus 120 degrees with respect to the electron beam. There was also 1-inch lead shielding in front of each HPGe detector to reduce the backscattered photon background. The results of the experiment are shown in Fig 2. The peaks labeled 1 – 9 are due to the ^{235}U NRF photons; their energies are specified in Table I. The additional, un-numbered peaks in the spectrum were due to the ^{235}U target casing material and were used for calibration purposes.

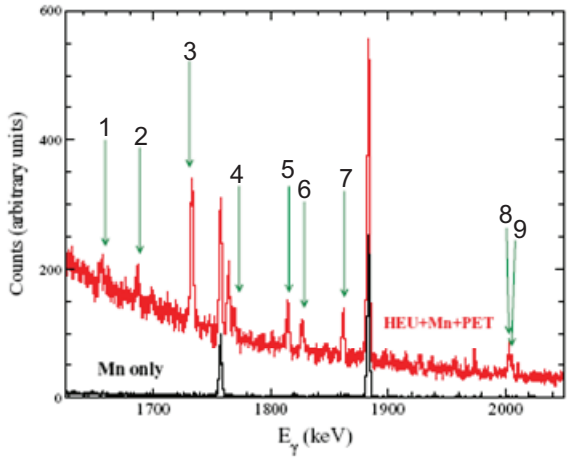

Fig. 2. Results of the experiment shown in Fig 1 and the energies of the nuclear resonances of ^{235}U from [3]. The numbers correspond the NRF resonance energies and cross sections listed in Table II.

TABLE I. MEASURED NRF DATA FROM [3].

Number	NRF Energy (keV)	Cross Section (eV-barns)
1	1656.23	4.1
2	1687.26	6.1
3	1733.60	29.8
4	1769.16	4.4
5	1815.31	9.7
6	1827.54	6.7
7	1862.31	9.6
8	2003.32	9.7
9	2006.19	4.7

III. SIMULATION METHODOLOGY

Initially the entire experimental setup was modeled using MCNPX, but the complete simulation proved too time-intensive. Also, as previously stated, the NRF cross sections do not exist in any publicly released version of MCNP. Because of this, a novel, multi-stage method was applied.

A. Simulation of the Bremsstrahlung Source

To simulate the backscattered photon spectrum the simulation was divided into three parts. The first part consisted of the generation of the bremsstrahlung spectrum in MCNPX. This model consisted only of the electron beam and the bremsstrahlung radiator. A diagram of the model is shown in Fig 3.

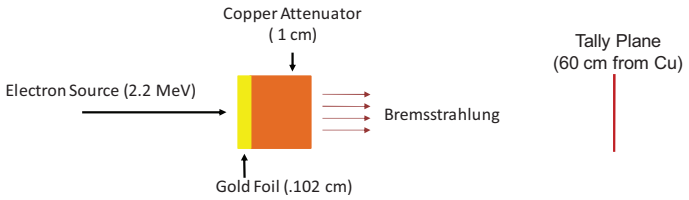

Fig. 3. Diagram of the MCNPX model used to generate the bremsstrahlung source.

A particle surface fluence tally (MCNPX F1) was placed 60 cm from the back of the copper attenuator to account for the angular distribution of the bremsstrahlung spectrum. Photons that were scattered at angles large enough to miss the NRF target were not transferred to the next stage of the simulation. The F1 tally from the simulation of the bremsstrahlung spectrum is shown in Fig 4. This spectrum was used as the source for the next step in the simulation procedure.

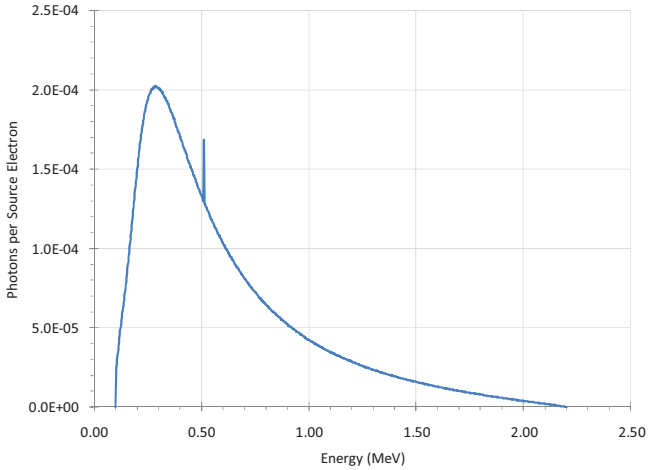

Fig. 4. Number of photons per source electron tallied 60 cm from the back face of the copper attenuator.

B. *Variance Reduction Verification*

The next step of the simulation involved the transport of the bremsstrahlung source to the target foil and tallying the backscattered photons that reach the surface of the lead shield. The bremsstrahlung source from the previous simulation is directed at the NRF target with a 2.5-degree half angle to account for the lead collimator used in the experiment. This simulation does not include the NRF emitted photons, only the backscattered source photons. This step of the simulation was the most time-intensive and necessitated the use of variance reduction techniques. A point detector tally (MCNPX F5) was placed in the center of the lead shielding front face. Fig. 5 shows an illustration of this portion of the simulation model. The lead shield and the HPGe detector were both voided to reduce the simulation time.

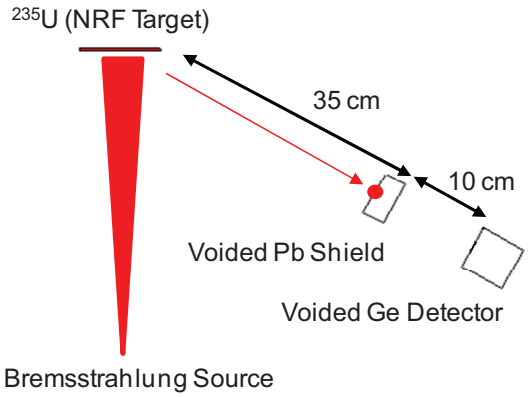

Fig. 5. MCNPX model used to compute the number of backscattered source photons crossing the lead shielding face.

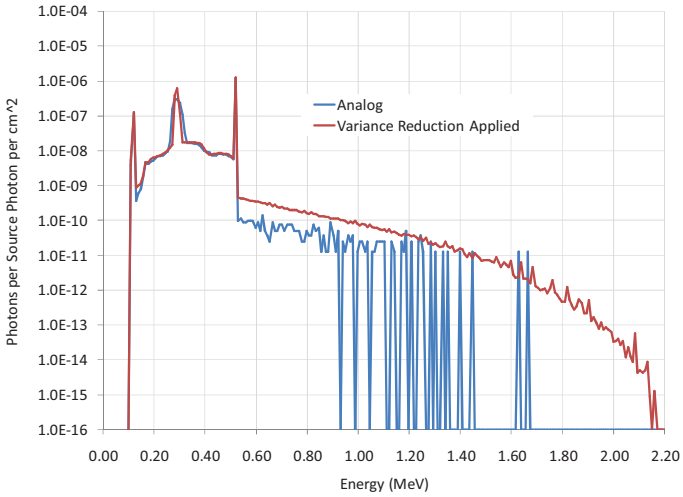

Fig. 6. Backscattered photons crossing the shielding face per source photon per cm^2 as a function of energy (MeV) crossing the front face of the lead shielding computed using analog (F1) and variance reduction tallies (F5).

The simulation was performed with and without variance reduction to verify that the variance reduction techniques were yielding accurate results. The results of both simulations are shown in Fig. 6. Based on the agreement between the two simulation in the energy range where the tallies were converges, it was concluded that the variance reduction techniques were accurately representing the analog results. Fig. 6 clearly illustrates the need for variance reduction in the energy range that is relevant to the experiment: between 1.6 and 2.1 MeV.

Upon comparing the MCNPX backscattered photon spectrum to the measurements of Bertozzi et al., it was discovered that there were large discrepancies. This has been primarily attributed to the fact that MCNP does not correctly account for Rayleigh (elastic) scattering of photons in the energy range and isotopes that are relevant to this analysis [4]. In fact, the Rayleigh scattering models in the current versions of MCNPX are the same as those implemented in the MCP code of 1973 [4]. The scattering cross section is a function of the momentum transfer in the interaction. However, the distributed versions of MCNP have a limited range of tabulated momentum values (based on the range of available data at the time on implementation). This presents a fundamental limitation on the energy range over which Rayleigh scattering is modeled; any scattering outside of the range is not modeled. Fig. 7 shows the fraction of Rayleigh scattering that is not modeled due to this cut-off in the tabulated data [4]. For ^{235}U, in the energy range considered here, only approximately 20% of the total Rayleigh scattering is actually modeled. Nowadays, the Evaluated Photon Data Library tabulates data over all relevant ranges; the models in MCNP need to be extended to accommodate them [4].

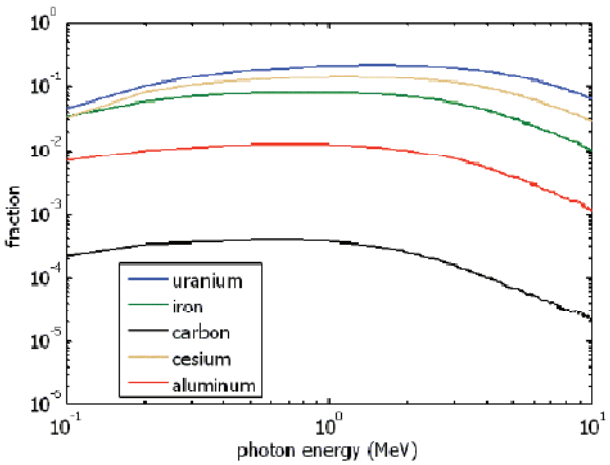

Fig. 7. Fractional Rayleigh scattering that is not modeled in the current versions of MCNPX due to a cut-off in the tabulated data (from [4]).

C. *Simulation of the NRF Emissions*

The NRF cross sections do not exist in any publicly released version of MCNP, so a novel method was employed to analyze the NRF component of the spectrum. The source was manually implemented into MCNPX, and the results were scaled in order to obtain a value of the number of counts in the detector per source photon. This was done for two different sources; the Bertozzi et al. bremsstrahlung source, and a 10% Gaussian source comparable to the predicted UNL Diocles-laser-driven X-ray source.

The model was performed in two stages. The first stage was simulated the number of NRF photons that reach the front face of the lead shielding. To determine the relative intensity of the NRF emission lines, the cross sections and source photon flux in the target were taken into consideration. The cross sections were weighted by the energy-dependant photon flux in the target. This resulted in the lower-energy resonances being weighted more heavily. Fig. 8 shows the bremsstrahlung flux in the NRF target as a function of energy and the NRF cross sections.

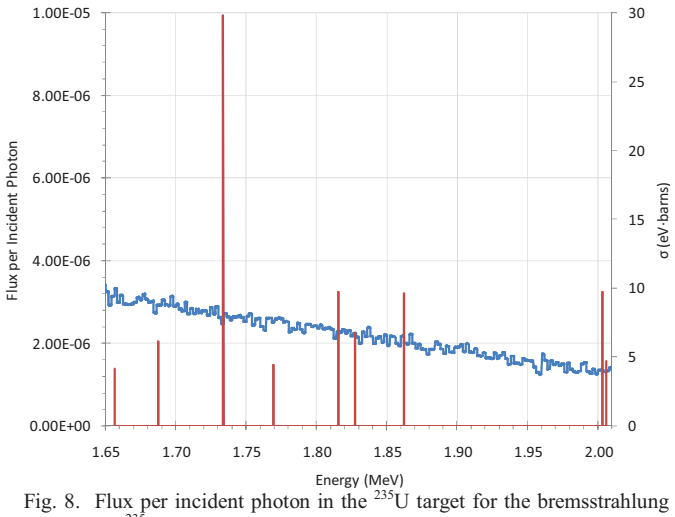

Fig. 8. Flux per incident photon in the ^{235}U target for the bremsstrahlung source and the ^{235}U resonance cross sections as a function of energy.

The bremsstrahlung flux in the target was obtained using a volume-averaged photon flux tally (MCNPX F4), and the cross sections data were taken from Bertozzi et al. as listed un Table I [3]. For the relative emission probability the following calculation was performed:

$$\mathrm{Pr}_{\text{NRF Emission}} = \varphi_{\text{NRF Energy}} \frac{\sigma_{\text{NRF Energy}}}{\sum_i \sigma_i} \qquad (1)$$

At each resonance energy, the cross section was divided by the total cross section and multiplied by the flux at that energy. The flux was assumed to be constant over the width of the resonance which is on the order of 10^{-1} eV. Using the probability of emission for each NRF peak, the NRF source lines were implemented into the MCNPX input file. The source was evenly distributed throughout the NRF target foil and emitted photons isotropically. Fig. 9 shows a diagram of the model used to simulate the number of photons that reach the shield per NRF emission. Again, the lead shield and the detector are voided to expedite the simulation and an F5 tally was used to compute the photon flux on the face of the lead shielding.

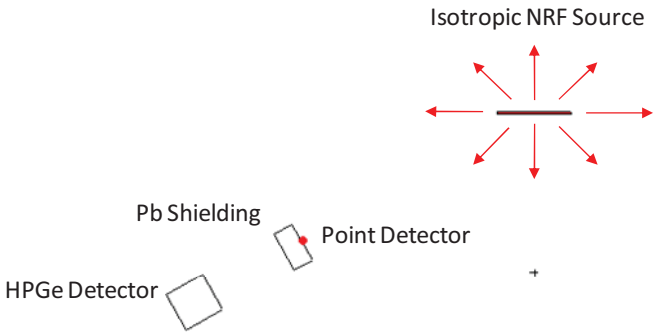

Fig. 9. Diagram of the simulation used to transport the NRF photons from the target to the front face of the lead shield. NRF source consists of all nine resonant photons. The model has identical dimensions to Fig. 5 and all cells are voided except the NRF target in order to expedite the simulation.

The F5 tally was then multiplied by the surface area of the detector in order to get the tally in units of NRF photons per source photon. Fig. 10 shows the results of the simulation and the subsequent scaling. This simulation takes into account the solid angle efficiency of the detector configuration.

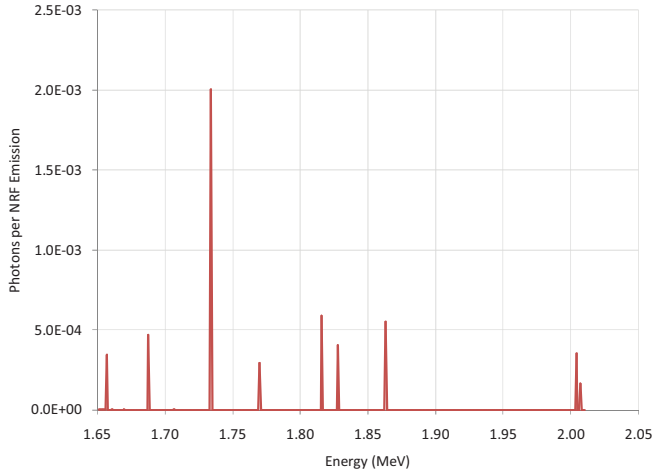

Fig. 10. Diagram of the simulation used to transport the NRF photons from the target to the front face of the lead shield.

The next stage of the simulation involves the transport of the photons incident on the lead through the lead and into the HPGe detector. A detector pulse height tally (MCNPX F8) was used to compute the number of counts in the detector per photon incident on the lead shield. The size of the detector and the lead shield were estimated from Fig. 1. The HPGe detector was a cylinder with a radius of 5.08 cm and a depth of 10.16 cm. The lead shield was estimated to be a cylinder with a radius of 5.08 cm and a depth of 2.54 cm. The incident NRF photons that crossed the front face of the lead were directed at the lead shield as a beam source. Fig. 11 shows a diagram of the simulation model.

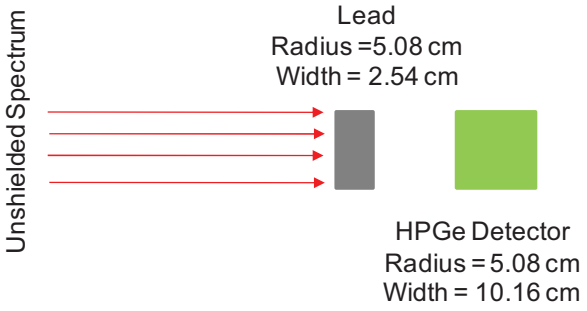

Fig. 11. Model of the simulation for the transport of the NRF photons tallied by the point detector through the lea shield

The results, shown in Fig. 12, take into account resolution of the detector by using the Gaussian Energy Broadening function in MCNPX. The spectrum shown in Fig. 12 was obtained by scaling the results from the previous stages. In order to obtain the number of counts per NRF emission the F8 tally had to be multiplied by the sum of the F5 tally and the surface area of the detector. Furthermore, to obtain the number of counts per source photon the, the number of counts per NRF emission must be multiplied by the number of NRF emissions per source photon as described in (2).

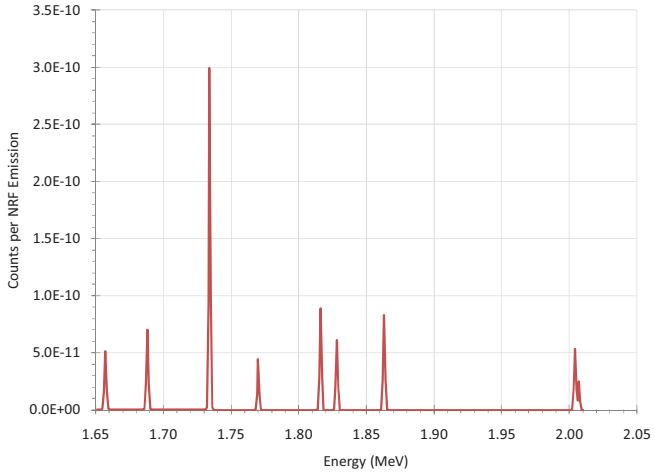

Fig. 12. Counts per NRF emission vs. energy for the bremsstrahlung source.

$$\frac{\text{Counts}}{\text{Source Photon}} = F8 \cdot F5 \cdot SA \cdot \frac{\text{NRF Emission}}{\text{Source Photon}} \tag{2}$$

The number of NRF emissions per source photon was calculated analytically:

$$\frac{\text{NRF Emissions}}{\text{Source Particle}} = N_{\text{NRF Target}} \cdot V_{\text{target}} \sum_i \{\sigma_i \varphi(E_i)\} \tag{3}$$

where $N_{\text{NRF Target}}$ is the atom density of the target foil, σ_i and φ_i are the NRF cross section and flux in the target foil corresponding to each NRF energy, and V_{Target} is the volume of the target foil.

The relative intensities of the simulated NRF lines were compared to the relative intensity of the experimental NRF in order to validate the simulation results. The number of counts above background for each measured NRF peak is listed in Table II. The peaks were then normalized to the most prominent peak (1733.60 keV). Fig. 13 shows the results. The relative heights of the peaks in each data set agree fairly well, especially when considering the uncertainty in the measured NRF cross sections which range from 13.1% to 34.0 % [3]. Further investigation will explore the affect of implementing these uncertainties into the MCNPX models on the NRF response.

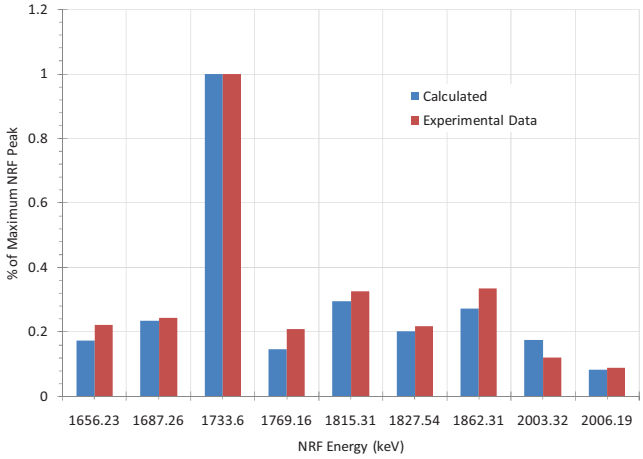

Fig. 13. Comparison of relative peak height for the experimental and simulated results.

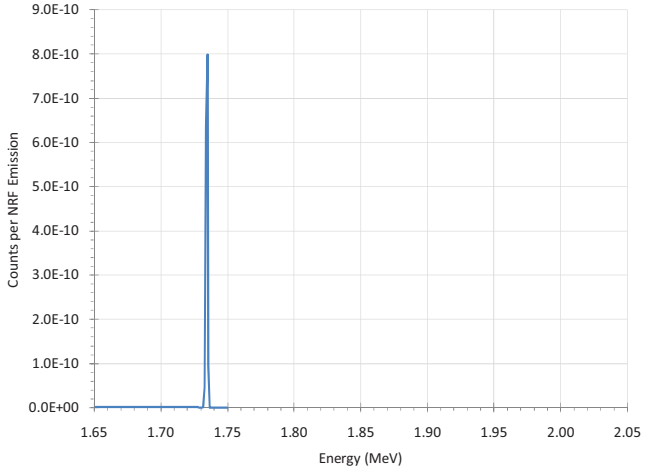

Fig. 14.Counts per NRF emission vs. energy for the 10% energy-spread Gaussian source.

TABLE II. MEASURED NRF CROSS SECTIONS AND COUNTS ABOVE BACKGROUND USED FOR VALIDATION OF THE MCNPX RESULTS.

Number	σ (eV•barns)	σ uncertainty (eV•barns)	Counts above Background
1	4.1	1.3	55
2	6.1	1.1	55
3	29.8	3.9	225
4	4.4	1.0	47
5	9.7	1.7	73
6	6.7	1.2	49
7	9.6	1.7	75
8	9.7	1.7	27
9	4.7	1.6	20

In order to compare the two sources on a per source photon basis, the number of integral counts per source photon in the 1733.60-keV NRF peak was calculated. A value of $3.9 \cdot 10^{-12}$ counts per source photon was obtained for the 1733.60-keV NRF peak using the bremsstrahlung source.

D. Simulation of the 10% Gaussian Source

The same procedure that was used for the bremsstrahlung source was used for the UNL quasi-monoenergetic source. A conical photon beam with a 2.5° half angle at 1733.60-keV with a 10% FWHM photon energy was used as the source. The number of counts per NRF emission was calculated and is shown in Fig. 14.

The number of counts per source photon was calculated to be $6.6 \cdot 10^{-10}$. This analysis indicates that the 10% Gaussian source is more efficient on a per photon basis by a factor of approximately 170 per source photon.

IV. SUMMARY AND CONCLUSIONS

As expected, the Gaussian source is more efficient than the bremsstrahlung source on a per source photon basis. This calculation does not take into account the intensity of the source. If the bremsstrahlung source is more intense than the 10% energy-spread Gaussian source by a sufficient amount it would be possible to get more NRF counts from the bremsstrahlung source over the same simulation time. Future work will be to evaluate the total NRF response for each typical source parameters including a more-realistic estimation of the backscattered contribution which will be made possible by a future version of MCNPX.

ACKNOWLEDGMENT

This material is based upon work supported by the U.S. Department of Homeland Security under Grant Award Number 2007-DN-077-ER0007-03. The views and conclusions contained in this document are those of the authors and should not be interpreted as necessarily representing the official policies, either expressed or implied, of the U.S. Department of Homeland Security.

REFERENCES

[1] N. J. Cunningham, S. A. Pozzi, S. D. Clarke, S. Banerjee, R. Vane, J. Beene, D. Shultz, and D. Umstadter (2008). *High-Energy Laser Accelerated Electron Beams for Long-Range Interrogation.* Transactions of the 20th International Conference on the Application of Accelerators in Research & Industry, August 10 – 15, Fort Worth, TX, USA.

[2] J. Pruet and C. Hagman. "Initial Design Calculations for a Detector System that will Observe Resonant Excitation of the 680 keV state in 238U", U.S. Department of Energy, Contract W-7405-Eng-48. UCRL-TR-227910, February 9, 2007.

[3] W. Bertozzi, J.A. Caggiano, M.S. Johnson, S.E. Korbly, R.J. Ledoux, D.P. McNabb, E.B. Norman, W.H. Park, and G.A. Warren. Nuclear Resonance Fluorescence Near 2 MeV in ^{235}U and ^{239}Pu. Physical Review. C 78, 041601® (2008).

[4] B. Quiter et al. Nondestructive Spent Fuel Assay Using Nuclear Resonance Fluorescence. Transactions of the 50th INMM Annual Meeting. July 12-16. Tuscon, AZ, USA.